Colloid Polym Sci (2013) 291:867–877
DOI 10.1007/s00396-012-2803-y

ORIGINAL CONTRIBUTION

Self-assembly behavior of fluorocarbon-end-capped poly (glycerol methacrylate) in aqueous solution

Zheng Li · Elkin Amado · Jörg Kressler

Received: 29 June 2012 / Revised: 31 August 2012 / Accepted: 4 September 2012 / Published online: 26 September 2012

Abstract Well-defined perfluoroalkyl-terminated poly (glycerol methacrylate) (R_F-PGMA) semitelechelics are prepared by atom transfer radical polymerization and copper(I)-catalyzed alkyne–azide cycloaddition reaction. R_F-PGMA has a similar architecture as the well-studied perfluorinated poly(ethylene oxide) (R_F-PEO) semitelechelics but bears two hydroxyl groups on each glycerol methacrylate unit. Because of the strong hydrophobic interaction of the perfluoroalkyl group, R_F-PGMA semitelechelics self-associate to form core–corona spherical micelles in water above the critical micellization concentration (cmc) which depends on poly(glycerol methacrylate) (PGMA) content and temperature. For comparison, the R_F-PEO semitelechelics with the same perfluoroalkyl terminal group as R_F-PGMA are also prepared. The cmc values of R_F-PGMA semitelechelics are found to increase with increasing temperature in water, which is opposite to the tendency of R_F-PEO semitelechelics. According to the thermodynamic studies, the micellization process of R_F-PGMA in aqueous solution is driven by both a negative enthalpy and an increase of entropy, whereas the micellization of R_F-PEO is an entropy-driven process exhibiting a positive micellization enthalpy. This striking different behavior originates from intra-/intermolecular hydrogen bonds between the hydroxyl groups of the PGMA chains. These strong inter- and intramolecular hydrogen bonds between PGMA segments lead to a self-aggregation of R_F-PGMA evident in temperature-dependent ^{1}H and ^{19}F NMR spectroscopy and dynamic light scattering measurements.

Keywords Self-assembly · Thermodynamics · Micellization · Semitelechelics · Poly(glycerol methacrylate)

Introduction

Fluorocarbon-modified water-soluble polymers (FMSPs) are one important class of hydrophobically modified water soluble polymers and possess unique properties due to the particular properties conferred by fluorinated moieties. Compared to hydrocarbon groups, the fluorocarbons are more stable, surface active, and hydrophobic [1–7]. A rule of thumb for the hydrophobicity of fluorinated block is that one CF_2 group is equivalent to 1.7 CH_2 groups [8]. These unique properties are caused by the fact that the fluorine atom has a large van der Waals radius, dense electron cloud, high ionization potential, and very low polarizability [1, 2]. Such characteristics make the FMSPs to have advantages in some aspects compared to their corresponding hydrocarbon analogs. For instance, FM poly(ethylene oxide) presents a higher viscosifying effect than the hydrocarbon-modified poly(ethylene oxide) (PEO) due to the stronger hydrophobic association [4].

It has been demonstrated that end-capped FMSPs (R_F-Ps) can adopt a variety of unique properties such as high solubility and biological activities, which may not be achieved in randomly fluorinated polymers and fluorinated block polymers [9, 10]. To date, a wide range of R_F-Ps including perfluorinated poly(ethylene oxide) (R_F-PEO) [2, 4–7], R_F-poly(*N*-isopropylacrylamide) (R_F-PNIPAM) [11, 12], R_F-poly(acrylic acid) [13, 14], and R_F-poly(*N*-acylethylene imine) [15], among others, has been prepared, and their

Electronic supplementary material The online version of this article (doi:10.1007/s00396-012-2803-y) contains supplementary material, which is available to authorized users.

Z. Li · E. Amado · J. Kressler (✉)
Department of Chemistry,
Martin Luther University Halle-Wittenberg,
Von-Danckelmann-Platz 4,
06120 Halle (Saale), Germany
e-mail: joerg.kressler@chemie.uni-halle.de

behavior in aqueous solution or at the air–water interface has been studied [4–15].

Poly(glycerol methacrylate) (PGMA) is a hydrophilic polymer which is applied for soft contact lenses, hydrogels, and other biomedical applications [16, 17]. In past decades, various PGMA-based amphiphilic or triphiphilic polymers have been prepared, and their aqueous solution properties have been investigated [18–20]. To the best of our knowledge, however, no attempt has been made to investigate the self-assembling behavior of perfluoroalkyl-terminated poly (glycerol methacrylate) (R_F-PGMA) in aqueous or organic solution. Whereas R_F-PEOs and R_F-PNIPAMs may show lower critical solution temperature behavior, R_F-PGMAs have the advantage of being water soluble at all temperatures, and as such, they are suitable candidates for applications where high temperatures may be a prerequisite.

With this in mind, we synthesized R_F-PGMA semitelechelics with the architecture composed of the PGMA main chain and a perfluoroalkyl group capped at one end, which could be considered as the analogs to the well-studied R_F-PEO semitelechelics. The R_F-PGMA semitelechelics are obtained by atom transfer radical polymerization (ATRP) followed by a copper(I)-catalyzed alkyne–azide cycloaddition reaction (CuAAC), also referred to as "click" chemistry. The degree of polymerization (DP) of PGMA varies from 14 to 113, whereas the perfluoroalkyl end group is always the same. The self-assembly behavior of R_F-PGMA semitelechelics in aqueous solution is investigated by various techniques including surface tension, isothermal titration calorimetry (ITC), NMR, and dynamic light scattering (DLS). Moreover, the thermodynamics of the micellization process of R_F-PGMA and R_F-PEO semitelechelics in water are compared.

Experimental section

Materials

All reagents are purchased from Sigma-Aldrich unless otherwise stated. Methoxypolyethylene glycol azide (M_n= 2,000 gmol^{-1}) ($PEO_{44}N_3$), 3-bromo-1-propanol (97 %), *N*,*N*,*N*-tributyl-1-butanaminium iodide (Bu_4NI), solketal (98 %), ammonium chloride (NH_4Cl, 99.5 %) dicyclohexano-18-crown-6 (97 %), methacryloyl chloride (Alfa Aesar, 97 %), sodium azide (NaN_3, 99.5 %), α-bromoisobutyryl bromide (98 %), hex-5-ynoic acid (97 %), nonadecafluoro-1-decanol (97 %), 4-(dimethylamino)pyridine (99 %), 2,2′-bipyridine (bpy), copper bromide (CuBr, 99.999 %), 1,4-dioxane (99 %), tetrahydrofuran (THF) (99.5 %), *n*-hexane (97 %), benzene (Roth, 99 %), acetone (98 %), trifluoroacetic acid (99 %), and ethanol (98 %) were used as received. Anisole (Alfa Aesar, 99 %), α,α,α-trifluorotoluene (98 %), 2-butanone (99 %), and triethylamine (Et_3N) (99.8 %) were dried overnight with CaH_2, distilled, and stored over molecular sieve.

Polymer synthesis

The azide functional ATRP initiator, 3-azidopropyl-2-bromoisobutyrate (APBIB), the alkyne functional perfluoroalkyl segment, nonadecafluoro-1-decyl hex-5-ynoate ($F_9C{\equiv}CH$), and the monomer, solketal methacrylate (SMA), were synthesized according to the procedures described elsewhere with some modifications (see online resource) [21–23]. The synthesis of perfluoroalkyl functional PGMA semitelechelics, abbreviated as $PGMA_xF_9$ (x is the DP of PGMA main chains; 9 represents the number of CF_2/CF_3 groups in perfluoroalkyl segment), involves the polymerization of the azide-terminated poly(solketal methacrylate)s ($PSMA_xN_3$) by ATRP using an azide-functionalized initiator, coupling the alkyne functional perfluoroalkyl segment with the $PSMA_xN_3$ via CuAAC and cleaving the ketal groups on the side chains of PSMA to afford $PGMA_xF_9$ (Scheme S1). The azide-terminated poly(solketal methacrylate)s were polymerized from SMA by ATRP at 50 °C using APBIB as initiator, copper bromide (CuBr) as catalyst, bpy as ligand, and anisole as solvent. After 20 h, the polymers were purified by column chromatography followed by precipitation into a cold excess of *n*-hexane. The different DP for the PGMA blocks is achieved by varying the molar ratio of SMA to initiator. The terminal N_3 group was coupled with $F_9C{\equiv}CH$ through CuAAC reaction [12] to form the hydrophilic triazole [24] and give the perfluoroalkyl-end-capped PSMA ($PSMA_xF_9$). Finally, the $PGMA_xF_9$ was obtained by acid hydrolysis of the $PSMA_xF_9$ in 1,4-dioxane. Pure $PGMA_xF_9$ was obtained by dialysis of the polymer aqueous solution against water using a multipurpose dialysis tubing (Spectra/Por 7 Membrane, molar mass cutoff = 1,000 Da) and freeze drying. The detailed experimental procedure for the polymer preparation is given in the online resource. The number-average molar mass (M_n) and PD values of the synthesized $PGMA_xF_9$ are summarized in Table 1. The $PEO_{44}F_9$ semitelechelic was prepared by attaching an $F_9C \equiv CH$ to the azide end group of $PEO_{44}N_3$ (44 is the number of repeating units) through CuAAC using the similar experiment condition as for the reaction in $PSMA_xF_9$. The chemical structure of synthesized polymers was confirmed by ^1H and ^{19}F NMR and FT-IR spectroscopy. $PSMA_xF_9$ was analyzed by size exclusion chromatography (SEC) in THF, and they have monomodal molar mass distributions and polydispersities around 1.2. The detailed spectra of polymers are shown in the online resource. Scheme 1 shows the chemical structure of the $PGMA_xF_9$ and $PEO_{44}F_9$ applied in this study.

Table 1 Polydispersities, molar masses, and cmc values for the $PGMA_xF_9$ semitelechelics

Polymers	M_w/M_n[a]	M_n ($g\,mol^{-1}$)[b]	cmc ($10^{-5}\,mol\,L^{-1}$)[c]
$PGMA_{14}F_9$	1.18	3,000	0.67
$PGMA_{40}F_9$	1.21	7,200	1.35
$PGMA_{85}F_9$	1.25	14,300	3.50
$PGMA_{113}F_9$	1.23	18,800	>10

[a] Obtained from SEC measurements on $PSMA_xF_9$ with THF as eluent and PMMA as standard

[b] Calculated from ^{1}H and ^{19}F NMR spectroscopy (see online resource)

[c] Obtained from surface tension measurement at 25 °C

Characterization

NMR spectroscopy

NMR measurements were performed on a Gemini 2000 spectrometer (Varian) operating at 400 MHz for ^{1}H and ^{19}F. The samples were prepared either in dimethyl sulfoxide-d_6 (DMSO-d_6) or in D_2O. The CF_3COOD was added as an internal standard for the ^{19}F NMR spectroscopy. The experimental conditions including concentration and temperature for each spectrum are indicated in the text.

Surface tension measurement

The surface tensions of aqueous solutions of the polymers at different concentrations were measured with a DCAT11 tensiometer (DataPhysics Instruments GmbH, Filderstadt, Germany) using the Wilhelmy plate method. The temperature was controlled by a circulating water bath system which is accurate to ±0.1 °C. The polymer concentration in the thermostated glass vessel was varied by the injection of aliquots of stock solution. Following each injection, the surface tension was then measured after 10 min of stirring and 1.5 h waiting period.

Isothermal titration calorimetry

ITC measurements were performed in a MicroCal VP-ITC (MicroCal, Inc., Southampton, MA). The sample cell (1.447 mL) was loaded with degassed Milli-Q water. The injection syringe (300 μL) was filled with degassed polymer aqueous solution. Polymer solution aliquots were injected in steps of 10 μL into the sample cell that was stirred by the rotating injection syringe at 320 rpm. The equilibration time after each injection was set to 300 to 900 s to allow the cell feedback system to return to the baseline. The reference power offset was 20 $\mu cal\ s^{-1}$. Data were evaluated with the ITC module for Origin software which is supplied by MicroCal, Inc.

Dynamic light scattering

All DLS measurements were carried out on a commercial apparatus of ALV-Laser Vertriebsgesellschaft GmbH, Langen, Germany. The light source was a vertically polarized green neodymium: YAG DPSS-200 laser (λ=532 nm) from Coherent, Auburn, CA, USA, with a power output of

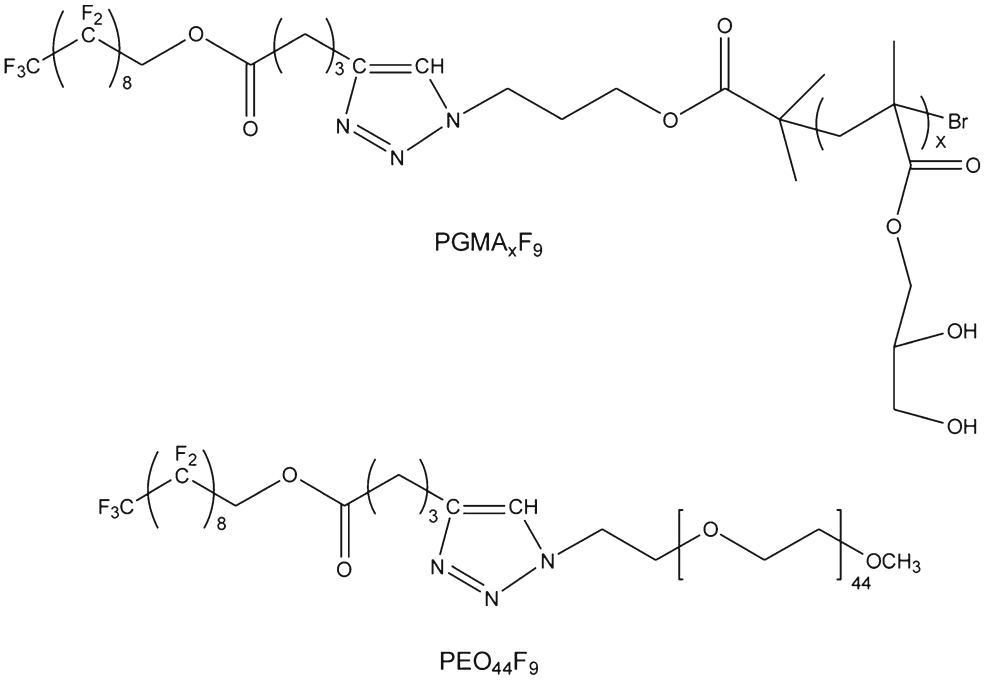

Scheme 1 The chemical structure of $PGMA_xF_9$ and $PEO_{44}F_9$ semitelechelics

200 mW. The samples were dissolved in Milli-Q water and then filtered through PTFE filters with 0.45-μm pore size in order to remove the dust. The R_h values were recorded for scattering angles from 50 to 130° after equilibrating the sample at the given temperature for 30 min. The average of two runs (60 s each) was recorded. The relative peak intensity is scaled with respect to the peak of the highest intensity which is put to an intensity of 1.

Results and discussion

It is well established that amphiphilic diblock copolymers, which consist of a long hydrophilic block and a relatively short hydrophobic block, associate into spherical micelles with a small dense core and a large-solvated corona above the critical micellization concentration (cmc) [25]. The cmc, defined as the copolymer concentration above which the formation of micelles becomes a dominant effect, is a fundamental parameter in characterizing the association properties of a given copolymer–solvent system [26]. Measuring the surface tensions over a wide range of concentrations is a commonly used method to determine the cmc. In an amphiphilic polymer–water system, the surface tension gradually decreases with increasing concentration due to the fact that hydrophobic polymer chains are adsorbed at the air–water interface. Once the polymer concentration reaches the cmc, the surface tension does not change significantly any more. The cmc is indicated by the intersection of the extrapolation of the two linear regimes where the curves show an abrupt change in the slope. The surface tension measurements were carried out at 25 °C using aqueous solutions of $PGMA_xF_9$, and the corresponding cmc data are summarized in Table 1. It is clearly evident that the cmc values show a significant increase with increasing PGMA content, since the longer soluble blocks usually carry higher "free energy cost" for being transferred from the unimer state to the micellar corona [27]. The measurements carried out at 25 °C using an aqueous solution of $PGMA_{113}F_9$ showed a continuous decrease of surface tension (γ) with increasing concentration, indicating that no micelles have been formed in the measured concentration range (Fig. S5).

The surface tension measurements of $PGMA_{40}F_9$ in aqueous solutions were carried out at 15, 25, 35, and 45 °C to investigate the temperature effect on the aggregation behavior. The cmc values obtained from the measurements are summarized in Table 2. Figure 1a represents the typical surface tensions obtained for $PGMA_{40}F_9$ in water as a function of polymer concentration at 15 and 45 °C. As can be seen from Fig. 1c, the cmc values exhibit a gradual increase with increasing temperature. At 45 °C, the cmc value of $PGMA_{40}F_9$ is about 1.5 times larger compared to the value at 15 °C. Such increase of the cmc with temperature is similar to the micellization of some block copolymers in an organic solvent, such as poly(styrene)-*b*-poly(tert-butylstyrene) in *N*,*N*-dimethylacetamide [28], since, in organic solvents, an increasing temperature usually improves the solvent quality for both blocks [29]. Amphiphilic polymers in aqueous solution usually show the opposite effect, that is, the cmc becomes smaller with increasing temperature. This is because the hydrocarbon usually becomes more hydrophobic at higher temperatures in water [29]. For comparison, the cmc values for $PEO_{44}F_9$ were measured at the same temperatures as for $PGMA_{40}F_9$. PEO is chosen as reference hydrophilic block for two reasons. The first is that hydrophobically end-capped PEOs have been widely studied, and thus, a large amount of data about their self-assembly behavior is available [30–32]. The second reason is that PEO has a significantly different chemical structure compared to PGMA. Figure 1b shows the surface tension measurements of $PEO_{44}F_9$ over a range of concentrations at 15 and 45 °C. The determined cmc values are summarized in Table 2. As expected, the cmc values show a gradual decrease with increasing temperature (Fig. 1c). This is in good agreement with the behavior of hydrophobically modified PEOs reported in literature [30–32].

Generally, the variation of the cmc values for amphiphilic substances in aqueous solutions is found to depend on the alteration of the interaction between the hydrophilic and/or hydrophobic blocks with water [29]. It should be noted that PGMA is a polymer rich in OH groups. When PGMA is dissolved in water, beside intermolecular hydrogen bonds between the polymer and water molecules, also inter-/intramolecular hydrogen bonds between and within the polymer chains can occur. An increase in temperature weakens the hydrogen bonding and has two opposite effects on the PGMA chain. On one hand, the increase of temperature may decrease hydrogen bonds between the PGMA and water molecules, which results in the dehydration of the PGMA block and favors the micellization. On the other hand, the increase of temperature can reduce the hydrogen-bonding effect between or within the PGMA polymer chains and make the PGMA chains more hydrated, which hinders micellization. In terms of magnitude, the endothermic enthalpy associated with the breaking of alkyl-OH–OH-alkyl interactions is smaller than the exothermic enthalpy associated with formation of alkyl-OH–HOH (hydration) [33]. The PGMA main chains become more hydrophilic at higher temperature because more inter- and intramolecular hydrogen bonds between and within the polymers are broken and more OH groups of the polymer chains become available for hydration. Meanwhile, with increasing temperatures, water becomes progressively a worse solvent for the hydrophobic block [29]. In other words, the hydrophobicity of the F_9 is enhanced, favoring micellization. From the data of the

Table 2 cmc and Gibbs free energy of micellization (ΔG^0_{mic}) of $PGMA_{40}F_9$ and $PEO_{44}F_9$ in aqueous solution at various temperatures

T (K)	$PGMA_{40}F_9$			$PEO_{44}F_9$		
	cmc (10^{-5} M)	$\Delta G^0_{mic}(kJmol^{-1})$	$\Delta S^0_{mic}(kJmol^{-1})$	cmc (10^{-5} M)	$\Delta G^0_{mic}(kJmol^{-1})$	$\Delta S^0_{mic}(kJmol^{-1}K^{-1})$
288	1.20	−36.7	0.087	1.55	−36.1	0.222
298	1.35	−37.7	0.087	1.05	−38.4	0.222
308	1.71	−38.4	0.087	0.68	−40.7	0.223
318	1.85	−39.4	0.087	0.52	−42.8	0.223

cmc values, it seems that the PGMA contribution dominates the cmc values at increasing temperatures and results in more hydrophilic $PGMA_xF_9$ semitelechelics at higher temperatures. In the case of $PEO_{44}F_9$, increasing temperature decreases the solvent quality for both the PEO and F_9 blocks and thus leads to a cmc decrease with increasing temperature. A similar increase on the hydrophilicity of the hydrophilic block in amphiphilic copolymers has also been observed by Halacheva et al. [34] They found that the cmc of poly(glycidol)-poly(propylene oxide)-poly(glycidol) (PG-PPO-PG) block copolymers is less temperature sensitive than their PEO-PPO-PEO analogs due to the weakening of the hydrogen bonding between the OH groups at the PG side chains [34].

The driving force for the micellization of the $PGMA_{40}F_9$ and $PEO_{44}F_9$ could also be identified from the thermodynamic parameters extracted from the cmc values at various temperatures. For a micellization process with significant

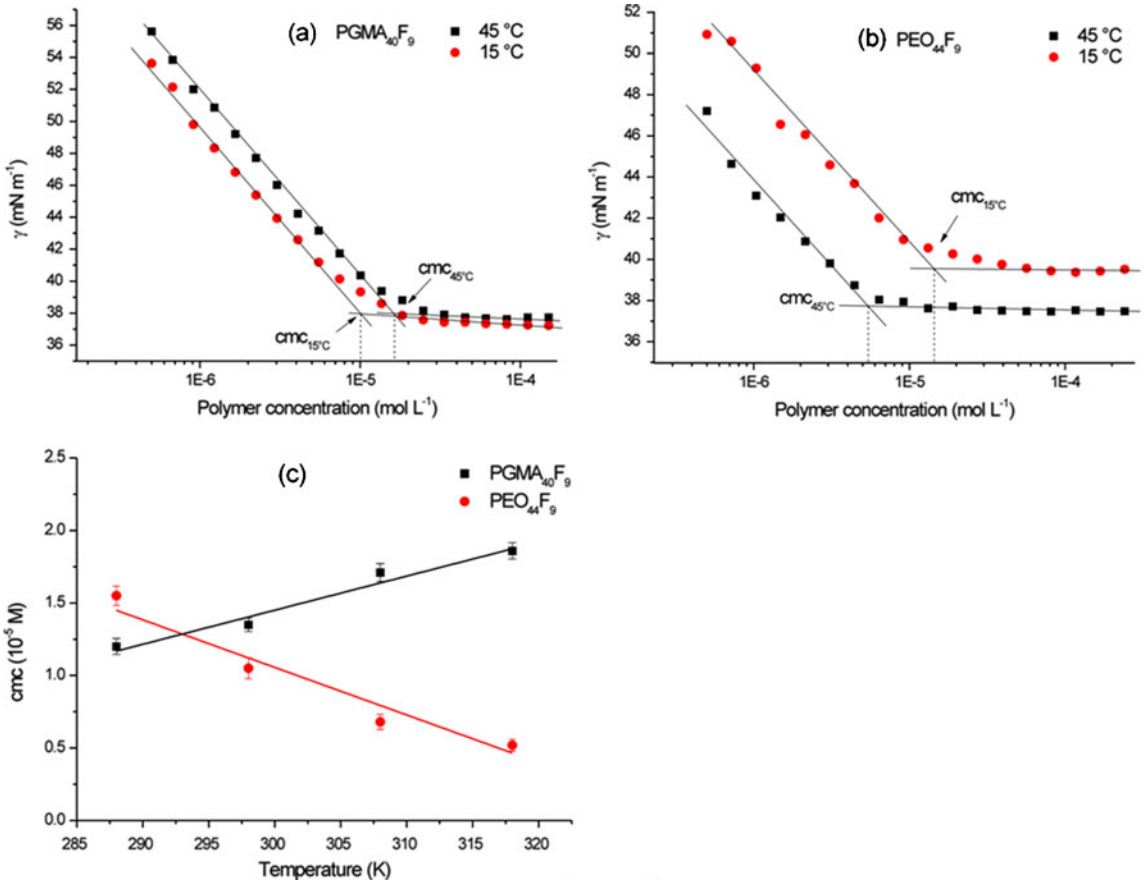

Fig. 1 Critical micellization concentration determination from surface tension measurements as a function of the concentration of **a** $PGMA_{40}F_9$ and **b** $PEO_{44}F_9$ at 15 and 45 °C. **c** The cmc values of $PGMA_{40}F_9$ and $PEO_{44}F_9$ at various temperatures

association number, the use of the relations below to calculate the standard free energy of micellization, ΔG^0_{mic}, and standard enthalpy of micellization, ΔH^0_{mic}, based on the cmc values is tolerable within experimental error [28, 35].

$$\Delta G^0_{mic} = RT\ln(X_{cmc}) \quad (1)$$

$$\Delta H^0_{mic} = R[dln(X_{cmc})/d(1/T)] \quad (2)$$

where R is the gas constant; T is the temperature in K, and X_{cmc} is the cmc in molar fraction at temperature T. Equation 2 can be integrated to yield the following:

$$\ln(X_{cmc}) = \Delta H^0_{mic}/RT + constant \quad (3)$$

provided that ΔH^0_{mic} is approximately a constant over the temperature range considered in this study. Figure 2 shows the van't Hoff plot for $PGMA_{40}F_9$ and $PEO_{44}F_9$ on the basis of Eq. 3. The slopes of the linear fits of the plots give $\Delta H^0_{mic}/R$ and lead to $\Delta H^0_{mic} = -11.7 \pm 1.5\ kJmol^{-1}$ for $PGMA_{40}F_9$, and $\Delta H^0_{mic} = 27.9 \pm 1.4\ kJmol^{-1}$ for $PEO_{44}F_9$. The standard entropy of micellization ΔS^0_{mic} can be obtained from the following:

$$\Delta S^0_{mic} = \left(\Delta H^0_{mic} - \Delta G^0_{mic}\right)/T \quad (4)$$

The values of ΔG^0_{mic}, and ΔS^0_{mic} for $PGMA_{40}F_9$ and $PEO_{44}F_9$ by this method are summarized in Table 2.

Both $PGMA_{40}F_9$ and $PEO_{44}F_9$ have positive ΔS^0_{mic} values. It is generally accepted that the gain in entropy during the micellization process arises from the release of water molecules in the hydration shells surrounding the hydrophobic groups [36]. Moreover, the mobility of the hydrophobic segments increases when they are removed from the aqueous solution into the core [37]. The positive ΔH^0_{mic} for $PEO_{44}F_9$ indicates that the micellization process is enthalpically not favored. This behavior is widely observed in the micellization of the amphiphilic polymers in aqueous solution. It is interesting to note that $PGMA_{40}F_9$ shows a negative ΔH^0_{mic}, i.e., its micellization process in aqueous solution is enthalpically favored. Thus, the micellization process of $PGMA_{40}F_9$ in aqueous solution is driven by both an increase in entropy and a negative micellization enthalpy.

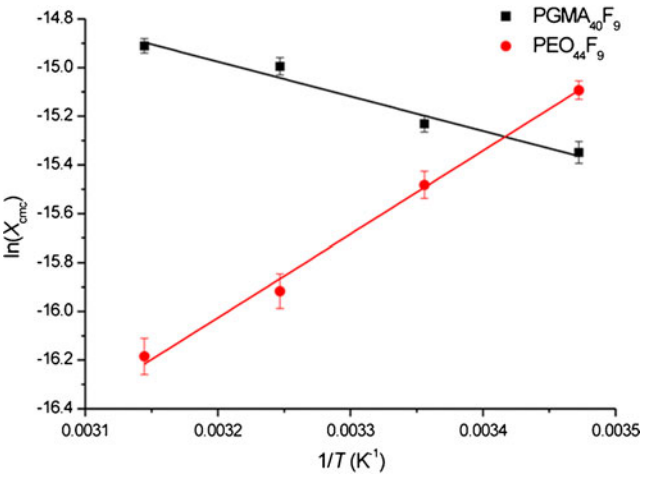

Fig. 2 Plots of the logarithmic cmc as a function of the reciprocal of the absolute temperature for $PEO_{44}F_9$ and $PGMA_{40}F_9$

It has been demonstrated that there are basically two contributions to the ΔH^0_{mic} in the micellization process of surfactants in aqueous solution. The first contribution arises from the transfer of the hydrophobic segments from the aqueous phase to the micelle core. This process is accompanied by a release of the water molecules surrounding the hydrophobic segments, which are structured differently from the water molecules in bulk, to the aqueous solution. This effect results in an exothermic enthalpy [36–38]. The second contribution is associated with the hydrophilic block. The hydrophilic repulsion due to the hydration and excluded volume forces of the hydrophilic chain give an endothermic contribution to ΔH^0_{mic} [38–40]. It is reasonable to conclude that the large difference in ΔH^0_{mic} found between $PEO_{44}F_9$ and $PGMA_{40}F_9$ comes from the hydrophilic blocks, since they share the same F_9 segments. The intra-/intermolecular hydrogen bonds in the PGMA blocks can weaken the hydration ability and decrease the excluded volume forces of the PGMA chains. In conclusion, the smaller endothermic contribution from the hydrophilic blocks of $PGMA_{40}F_9$ during micellization leads to a more exothermic ΔH^0_{mic} compared to that of $PEO_{44}F_9$.

ITC directly measures the heat effects accompanying association or disassociation between molecular entities [41]. For the association behavior of a surfactant in solution, ITC has the advantage that the cmc and ΔH^0_{mic} can be determined directly. To obtain further information on the micellization of $PGMA_{40}F_9$ and $PEO_{44}F_9$ in aqueous solution, ITC experiments are carried out at 20 °C. In a typical measurement, small aliquots of stock polymer solution are injected into water kept in the titration cell of the calorimeter at constant temperature. The heat evolved after each injection is registered as a peak, and the area under each peak is calculated for the different polymer concentrations in the titration cell.

Figure 3 shows the demicellization enthalpograms with the heat per injection as a function of polymer concentration during the titration of 1 mM $PGMA_{40}F_9$ (a) and 1 mM $PEO_{44}F_9$ aqueous solution (b) to water. The titration curves of these two samples are shown in Fig. S6 (online resource). The enthalpograms of both semitelechelics do not show a sigmoidal shape but, instead, exhibit a gradual change of enthalpy with polymer concentration caused by the fact that they assemble via a noncooperative process. Such a phenomenon is common in the self-assembly of polymers [42,

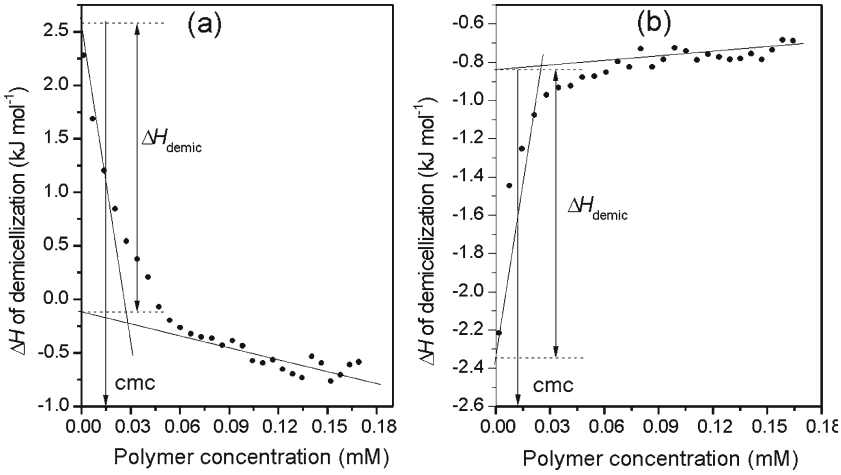

Fig. 3 The integrated heat per injection (normalized with respect to the injected number of moles of polymer) as a function of the total concentration of **a** $PGMA_{40}F_9$ and **b** $PEO_{44}F_9$ in the sample cell

43]. The demicellization enthalpograms can be subdivided into two concentration regions and reflect different processes. In the low concentration region, a large enthalpic effect is observed to be attributed to the dilution of micelles, demicellization of micelles, and dilution of unimers. The semitelechelics' concentration in the sample cell is below the cmc, and the micelles of the injected aliquots disaggregate completely. At polymer concentrations in the calorimeter cell above the cmc, the measured heat comes only from the dilution of micelles. The cmc values are determined by taking the concentration value at the half-height of the enthalpogram, and the cmc values of $\sim 1.4\times10^{-5}$ and $\sim 1.1\times10^{-5}$M are obtained for $PGMA_{40}F_9$ and $PEO_{44}F_9$, respectively. Figure 3 confirms that the $PGMA_{40}F_9$ exhibits an exothermic micellization process, whereas an endothermic micellization process is observed for $PEO_{44}F_9$. As illustrated in Fig. 3, the enthalpy of micellization, ΔH^0_{mic}, is determined according to a method described by Winnik et al. [42]. The ΔH^0_{mic} determined for $PGMA_{40}F_9$ and $PEO_{44}F_9$ at 20 °C are −2.72 and 1.62 kJmol^{-1}, respectively. It should be mentioned that the ΔH^0_{mic} values for both polymers obtained from the ITC measurements are smaller in magnitude compared to those estimated from the temperature-dependent cmc measurement (~−11.7 kJ mol^{-1} for $PGMA_{40}F_9$ and ~27.9 kJmol^{-1} for $PEO_{44}F_9$). In fact, ΔH^0_{mic} determined from ITC is always found to be significantly smaller than that estimated from temperature-dependent cmc measurement [35, 44]. This difference may be due to the distribution of chain lengths of polymers. The ΔH^0_{mic} from ITC relates to the whole sample, whereas that >from temperature-dependent cmc measurements only relate to the polymer fraction present in higher amount [35]. Even so, the ΔH^0_{mic} obtained from the ITC measurements reflects the

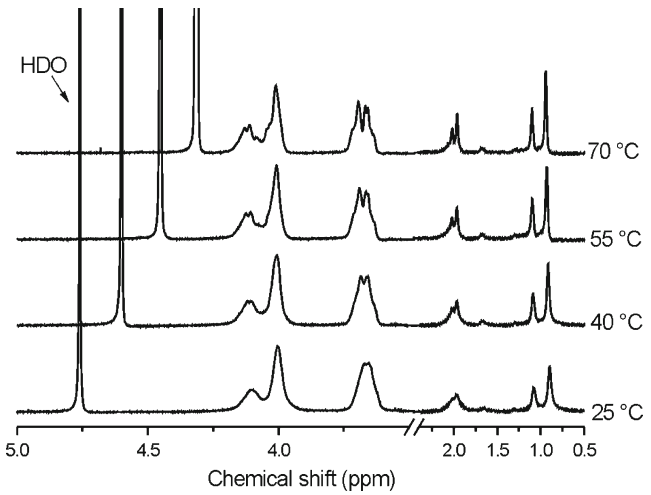

Fig. 4 Effect of temperature on the ^{1}H NMR spectra of 1.5 mM $PGMA_{40}F_9$ in D_2O at 400 MHz

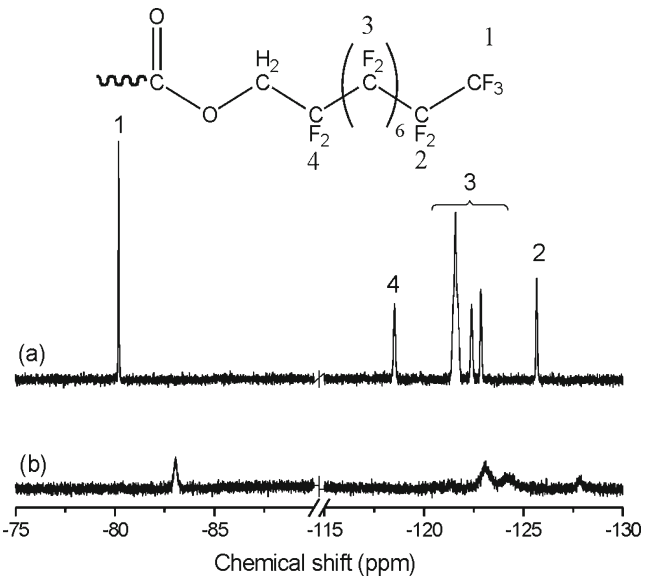

Fig. 5 ^{19}F NMR spectra of 1.5 mM $PGMA_{40}F_9$ at 25 °C and 400 MHz, in **a** DMSO-d_6 and in **b** D_2O

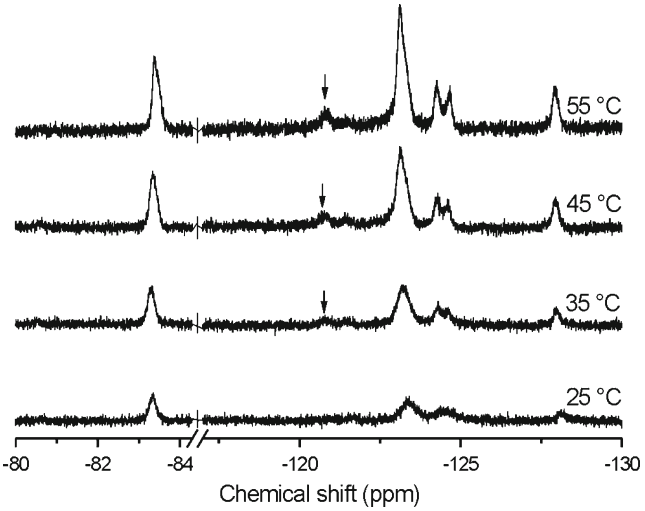

Fig. 6 Effect of temperature on the ^{19}F NMR spectra of 1.5 mM $PGMA_{40}F_9$ in D_2O at 400 MHz

same trend in sign as those estimated from the temperature-dependent cmc measurements.

Figure 4 compares the systematic changes in the ^1H NMR spectra of $PGMA_{40}F_9$ recorded at 25, 40, 55, and 70 °C in D_2O. The temperature-dependent residual HDO resonance signal is corrected for each temperature according to the studies by Gottlieb et al. [45]. The resonance bands of OH groups on the side chains of PGMA do not appear in the spectra because of the D/H exchange (the assignment is shown in the online resource). Examination of Fig. 4 shows that the resolution of the resonance signals is gradually improved with increasing temperature. For instance, the band at ~3.6 ppm, which is attributed to the methylene group adjacent to the OH on the PGMA side chains, shows a distinct hyperfine structure at 70 °C. This hyperfine structure progressively broadens with decreasing temperature and completely disappears at 25 °C. This observation indicates that the mobility of the PGMA chains increases with temperature. Such behavior can be attributed to the weakening of the hydrogen bonding involving the OH groups on the GMA units with increasing temperature, resulting in increasing solubility and mobility of the PGMA segments in aqueous solution.

^{19}F NMR spectroscopy is a powerful tool to investigate the self-assembly behavior of fluorocarbon-containing polymers, since the chemical shift of fluorine nuclei is very sensitive to changes of the environment [46, 47]. Figure 5 shows the ^{19}F NMR spectra of $PGMA_{40}F_9$ recorded in (a) DMSO-d_6 and (b) D_2O with a polymer concentration of ~1.5 mM at 25 °C. Six sharp and well-resolved resonance signals are observed and assigned in the ^{19}F NMR spectrum recorded in DMSO-d_6, since it is a nonselective solvent for the semitelechelic, and the F_9 segments exposed directly to the solvent. However, only four weak, broader, and attenuated resonance signals are observed in the spectrum recorded in D_2O. The peaks attributed to the CF_2 units numbered as "3", which appear as three well-separated peaks in DMSO-d_6, show only two attenuated peaks in D_2O. The peak of the CF_2 unit numbered as "4" closest to the PGMA segment completely disappeared. Furthermore, the comparison of Fig. 5a, b shows that all the peaks shift to lower chemical shift in D_2O than those in DMSO-d_6. For instance, the peak of the trifluoromethyl group (CF_3) at the end of the F_9 segments appears at~−80.0 ppm in DMSO-d_6 whereas at~−83.3 ppm in D_2O. Generally, the upfield shift of the peaks suggests the more shielded nuclei [3]. It is reasonable considering that the fluorine nuclei are transferred into a fluorocarbon-rich environment rather than in D_2O. This evidence clearly demonstrates that polymeric micelles with F_9 segments as the core are formed for the $PGMA_{40}F_9$ in D_2O. The resonance peak at~−83.3 ppm shown in D_2O is considered as the characteristic signal of CF_3 in the aggregated state [2, 3]. Moreover, both CF_3 resonance signals attributed to the unimer and associated polymer at the chemical shift of~−80.0 ppm and~−83.3 ppm, respectively, can be observed in the spectra of $PGMA_{85}F_9$ and $PGMA_{113}F_9$ in D_2O, which is discussed in online resource (Fig. S7).

To verify the effect of temperature on the aggregation behavior of the F_9 segment, the ^{19}F NMR spectra of $PGMA_{40}F_9$ are recorded in D_2O at 25, 35, 45 and 55 °C. These spectra are depicted in Fig. 6. Similar as the temperature-dependent ^1H NMR spectra discussed above, the resolution of the spectrum is gradually improved with increasing temperature. At 25 °C, there are only four broad

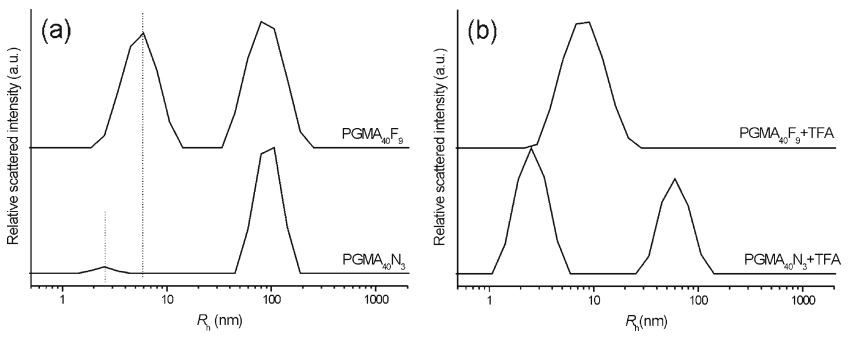

Fig. 7 DLS results of **a** $PGMA_{40}F_9$ and $PGMA_{40}N_3$ in water at 288 μM at 25 °C, θ=90° and **b** with the addition of 0.2 M TFA

and attenuated resonance peaks shown in the spectrum. Upon increasing the temperature to 55 °C, six resonance signals are considerably resolved similar to the spectrum in DMSO-d_6. Specifically, the signal from the CF_2 unit closest to the PGMA block labeled as number "4" in Fig. 5a, which is not seen at 25 °C, appears at 35, 45, and 55 °C (see arrows in Fig. 6). In the literature, such increase in signal resolution has been attributed to increasing mobility of the fluorocarbon moieties [6].

Figure 7a shows the size distributions of 288 μM aqueous solutions of $PGMA_{40}N_3$ and $PGMA_{40}F_9$ semitelechelics at 25 °C obtained from DLS measurements. Two relaxation modes are observed in $PGMA_{40}N_3$ and $PGMA_{40}F_9$ aqueous solutions. The fast modes with R_h of ~2.5 nm in $PGMA_{40}N_3$ and ~6 nm in $PGMA_{40}F_9$ are considered to belong to the unimers and polymeric micelles, respectively, in agreement with the expected particle sizes for unimers and micelles. Concentration-dependent DLS measurements for $PGMA_{40}F_9$ exhibit similar bimodal distributions with a fast mode corresponding to micelles above cmc and to unimers below cmc (Fig. S8, online resource). It has been reported that interpolymer complexes can be formed by secondary-binding forces including van der Waals forces, hydrophobic interactions, electrostatic interactions, and hydrogen bonding [48, 49]. Polymer hydrogen-bonding complexes have been observed in many donor/acceptor-containing polymers, such as the OH-bearing polymers [50]. Recently, PGMA homopolymer and block copolymer chains were reported to show high affinity to each other to form clusters via intermolecular hydrogen bonding between the OH [19, 20]. It is, therefore, reasonable to conclude that intermolecular hydrogen bond is responsible for the polymer clusters with the R_h of ~105 nm in $PGMA_{40}N_3$ aqueous solution. The slow mode with R_h of ~90 nm in $PGMA_{40}F_9$ aqueous solution is related to clusters of micelles. Such micellar clusters has been observed also in aqueous solutions of diblock copolymers based on PEO [51]. When two micelles come into contact, there is an overlapping region where polymer chains can interpenetrate and squeeze out some solvent molecules [51, 52]. The interpenetration of PGMA chains provides a possibility to form intermolecular hydrogen bonding between coronae of $PGMA_xF_9$ micelles.

The hydrogen-bonding effect in $PGMA_xF_9$ is further confirmed by the addition of trifluoroacetic acid (TFA), a commonly used hydrogen bond breaker. Figure 7b shows the size distributions of 288 μM $PGMA_{40}F_9$ and $PGMA_{40}N_3$ aqueous solution with 0.2 M TFA. After adding TFA, the slow mode was significantly suppressed in both PGMA homopolymer and semitelechelic. For $PGMA_{40}N_3$ with TFA, the amplitude ratio of the scattering intensity of the fast mode to the slow mode exhibits a strong increase compared to the solutions without TFA, suggesting that the number of the polymer clusters is largely reduced. In $PGMA_{40}F_9$, the slow mode disappeared completely after the addition of TFA. Moreover, the R_h of the $PGMA_{40}F_9$ micelles increases from ~6 to ~8 nm. This can be attributed to the fact that polymer micelles become less compact due to the weakening of inter- and intramolecular hydrogen bonding.

Conclusions

In this study, perfluoroalkyl-end-capped PGMAs and PEO semitelechelics were prepared, and their self-assembly in water was investigated. $PGMA_{40}F_9$ showed a different association behavior in aqueous solution compared to the analog $PEO_{44}F_9$ as follows: (1) the cmc values of $PGMA_{40}F_9$ increased gradually with increasing temperature, while $PEO_{44}F_9$ showed the opposite tendency, as determined from surface tension measurements. (2) The thermodynamic parameters, ΔH^0_{mic} and ΔS^0_{mic}, calculated from the cmc values at different temperatures showed that the micellization process of $PGMA_{40}F_9$ in aqueous solution was driven by both a negative enthalpy and an increase in entropy. Meanwhile, the micellization of $PEO_{44}F_9$ was an entropy-driven process. The same trend was also observed in ITC measurements. These significant differences resulted from the partial self-association through hydrogen bonds, which occurs among the PGMA segments.

It is interesting to note that the thermodynamics of the micellization of $PGMA_{40}F_9$ in water was different compared to the commonly used semitelechelics. This study contributes to a better understanding of the self-assembly process of semitelechelics which have strong affinity to self-aggregation via hydrogen bonds.

Acknowledgments Authors would like to thank for financial support by DFG (FOR 1145).

References

1. Amado E, Kressler J (2011) Triphilic block copolymers with perfluorocarbon moieties in aqueous systems and their biochemical perspectives. Soft Matter 7:7144–7149. doi:10.1039/C1SM05339F
2. Hoang KC, Mecozzi S (2004) Aqueous solubilization of highly fluorinated molecules by semifluorinated surfactants. Langmuir 20:7347–7250. doi:10.1021/la049128a
3. Hwang FS, Hogen-Esch TE (1995) Effects of water-soluble spacers on the hydrophobic association of fluorocarbon-modified poly(acrylamide). Macromolecules 28:3328–3335. doi:10.1021/ma00113a037
4. Zhang HS, Pan J, Hogen-Esch TE (1998) Synthesis and characterization of one-end perfluorocarbon-functionalized derivatives of poly(ethylene glycol)s. Macromolecules 31:815–2821. doi:10.1021/ma9712256

5. Amado E, Kressler J (2005) Synthesis and hydrolysis of α, ω-perfluoroalkyl-functionalized derivatives of poly(ethylene oxide). Macromol Chem Phys 206:850–859. doi:10.1002/macp.200400535
6. Preuschen J, Menschen S, Winnik MA, Heuer A, Spiess HW (1999) Aggregation behaviour of a symmetric, fluorinated, telechelic polymer system studied by ^{19}F NMR relaxation. Macromolecules 32:2690–2695. doi:10.1021/ma9818735
7. Boschet F, Branger C, Margaillan A, Condamine E (2002) Synthesis, characterisation and aqueous behaviour of one-ended perfluorocarbon-modified poly(ethylene glycol). Polymer 43:5329–5334. doi:10.1016/S0032-3861(02)00397-X
8. Racey JC, Stébé J (1994) Properties of fluorinated non-ionic surfactant-based systems and comparison with non-fluorinated systems. Colloid Surf A: Physiochem Eng Aspects 84:11–31. doi:10.1016/0927-7757(93)02731-S
9. Sawada H (2000) Architecture and applications of novel self-assembled aggregates of fluoroalkyl-end-capped oligomers. J Fluorine Chem 101:315–324. doi:10.1016/S0022-1139(99)00177-3
10. Sawada H (2000) Chemistry of fluoroalkanoyl peroxides, 1980–1998. J Fluorine Chem 101:219–220. doi:10.1016/S0022-1139(00)00279-7
11. Li M, Jiang M, Zhang YX, Fang Q (1997) Fluorescence studies of hydrophobic association of fluorocarbon-modified poly(*N*-isopropylacrylamide). Macromolecules 30:470–478. doi:S0024-9297(96)00966-7
12. Li Z, Kyeremateng SO, Fuchise K, Kakuchi R, Sakai R, Kakuchi T, Kressler J (2009) Aggregation behavior of poly(*N*-isopropylacrylamide) semitelechelics with a perfluoroalkyl segment in water. Macromo Chem Phys 21:2138–2147. doi:10.1002/macp.200900334
13. Chen JY, Jiang M, Zhang YX, Zhou H (1999) Fluorescence studies on hydrophobic associations of fluorocarbon-modified modified poly(acrylic acid) solutions. Macromolecules 32:4861–4866. doi:10.1021/ma9816160
14. Zhuang DQ, Hogen-Esch TE, Zhang YX (2004) Rheological investigation on the interaction of a fluorocarbon and hydrocarbon comodified PAA with a nonionic surfactant in the presence of salt. J Applied Polym Sci 92:1279–1285. doi:10.1002/app.20080
15. Kubowicz S, Thünemann AF, Weberskirch R, Möhwald H (2005) Cylindrical micelles of alpha-fluorocarbon-omega-hydrocarbon end-capped poly(*N*-acylethylene imine)s. Langmuir 21:7214–7219. doi:10.1021/la050987o
16. Gates G, Harmon JP, Ors J, Benz P (2003) Intra and intermolecular relaxations 2,3-dihydroxypropyl methacrylate and 2-hydroxyethyl methacrylate hydrogels. Polymer 44:207–214. doi:10.1016/S0032-3861(02)00725-5
17. Leung BK, Robinson GB (1993) The structure of crosslinked poly (glyceryl methacrylate) hydrogel networks. J Appl Polym Sci 47:1207–1214. doi:10.1002/app.1993.070470708
18. Amado E, Augsten C, Mäder K, Blume A, Kressler J (2006) Amphiphilic water soluble triblock copolymers based on poly (2,3-dihydroxypropyl methacrylate) and poly(propylene oxide): synthesis by atom transfer radical polymerization and micellization in aqueous solutions. Macromolecules 39:9486–9496. doi:10.1021/ma060794n
19. Kyeremateng SO, Henze T, Busse K, Kressler J (2010) Effect of hydrophilic block-a length tuning on the aggregation behavior of α, ω-perfluoroalkyl end-capped ABA triblock copolymers in water. Macromolecules 43:2502–2511. doi:10.1021/ma902753y
20. Kyeremateng SO, Busse K, Kohlbrecher J, Kressler J (2011) Synthesis and self-organization of poly(propylene oxide)-based amphiphilic and triphilic block copolymers. Macromolecules 44:583–593. doi:10.1021/ma102232z
21. Urien M, Erothu H, Cloutet E, Hiorns RC, Vignau L, Cramail H (2008) Poly(3-hexylthiophene) based block copolymers prepared by "click" chemistry. Macromolecules 41:7033–7040. doi:10.1021/ma800659a
22. Kyeremateng SO, Amado E, Kressler J (2007) Synthesis and characterization of random copolymers of (2,2-dimethyl-1,3-dioxolan-4-yl)methyl methacrylate and 2,3-dihydroxypropyl methacrylate. Eur Polym J 43:3380–3391. doi:10.1016/j.eurpolymj.2007.04.048
23. Golas PL, Tsarevsky NV, Sumerlin BS, Matyjaszewski K (2006) Catalyst performance in "click" coupling reactions of polymers prepared by ATRP: ligand and metal effects. Macromolecules 39:6451–6457. doi:10.1021/ma061592u
24. Reuter S, Busse K, Radics U, Niclas HJ, Kressler J (2009) Langmuir monolayers and Langmuir-Blodgett films of 1-acyl-1,2,4-triazoles. J Colloid Interface Sci 340:276–284. doi:10.1016/j.jcis.2009.08.046
25. Hamley IW (1998) In the physicals of block copolymers. Oxford University Press, Oxford
26. Chu B, Zhou ZK (1996) Physical chemistry of polyoxyalkylene block copolymer surfactants. In: Nace VM (ed) Nonionic surfactants: polyoxyalkylene block co-polymer studies. Marcel Dekker, New York
27. LaRue I, Adam M, Zhulina E, Rubinstein M, Pitsikalis M, Hadjichristidis N, Ivanov D, Gearba RI, Anokhin DV, Sheiko SS (2008) Effect of the soluble block size on spherical diblock copolymer micelles. Macromolecules 41:6555–6563. doi:10.1021/ma800403r
28. Zhou ZK, Chu B, Peiffer DG (1993) Temperature-induced micelle formation of a diblock copolymer of styrene and tert-butylstyrene in N, N-dimethylacetamide. Macromolecules 26:1876–1883. doi:10.1021/ma00060a013
29. Alexandridis P, Lindman B (2000) Amphiphilic block copolymers, self-assembly and application. Elsevier, Amsterdam
30. Dai S, Tam KC (2003) Isothermal titration calorimetric studies of alkyl phenol ethoxylate surfactants in aqueous solutions. Colloids and Surfaces A: Physicochem Eng Aspects 229:157–168. doi:10.1016/j.colsurfa.2003.09.007
31. Olofsson G (1985) Microtitration calorimetric study of the micellization of three poly(oxyethylene)glycol dodecyl ethers. J Phys Chem 89:1473–1477. doi:10.1021/j100254a034
32. Mai SM, Booth C, Kelarakis A, Havredaki V, Ryan AJ (2000) Association and surface properties of poly(ethylene oxide)–poly (styrene oxide) diblock copolymers in aqueous solution. Langmuir 16:1681–1688. doi:10.1021/la991004o
33. Graziano G (1999) Hydration thermodynamics of aliphatic alcohols. Phys Chem Chem Phys 1:3567–3576. doi:10.1039/A903082D
34. Halacheva S, Rangelov S, Tsvetanov C (2006) Poly(glycidol)-based analogues to pluronic block copolymers. synthesis and aqueous solution properties. Macromolecules 39:6845–6852. doi:10.1021/ma061040b
35. Taboada P, Mosquera V, Attwood D, Yang Z, Booth C (2003) Enthalpy of micellization of a diblock copoly(oxyethylene/oxypropylene) by isothermal titration calorimetry. Comparison with the van't Hoff value. Phys Chem Chem Phys 5:2625–2627. doi:10.1039/b303108j
36. Tanford C (1973) The hydrophobic effect. Wiley, New York
37. Grosmaire L, Chorro M, Chorro C, Partyka S, Zana R (2002) Alkanediyl-α, ω-bis(dimethylalkylammonium bromide) surfactants: 9. Effect of the spacer carbon number and temperature on the enthalpy of micellization. J Colloid Interface Sci 246:175–181. doi:10.1006/jcis.2001.8001
38. Pestman JM, Kevelam J, Blandamer MJ, von Doren HA, Kellogg RM, Engberts JBFN (2009) Thermodynamics of micellization of nonionic saccharide-based *N*-acyl-*N*-alkylaldosylamine and *N*-acyl-*N*-alkylamino-1-deoxyalditol surfactants. Langmuir 15:2009–2014. doi:10.1021/la981404w

39. Moroi Y, Nishikido N, Uehara H, Matura R (1975) An interrelationship between heat of micelle formation and critical micelle concentration. J Colloid Interface Sci 50:254–263. doi:10.1016/0021-9797(75)90228-3
40. Corkill JM, Goodman JF, Tate JR (1968) Hydrogen-bonded solvent. Ayst Proc Symp 1968:181
41. Okhrimenko O, Jelesarov L (2008) A survey of the year 2006 literature on applications of isothermal titration calorimetry. J Mol Recongnit 21:1–19. doi:10.1002/jmr.859
42. Raju BB, Winnik FM, Morishima Y (2001) A look at the thermodynamics of the association of amphiphilic polyelectrolytes in aqueous solutions: strengths and limitations of isothermal titration calorimetry. Langmuir 17:4416–4421. doi:10.1021/la001554i
43. Kujawa P, Goh CCE, Calvet D, Winnik FM (2001) Do fluorocarbon, hydrocarbon, and polycyclic aromatic groups intermingle? Solution properties of pyrene-labeled bis(fluorocarbon/hydrocarbon)-modified poly(*N*-isopropylacrylamide). Macromolecules 34:6387–6395. doi:10.1021/ma010384t
44. Taboada P, Velasquez G, Barbosa S, Yang Z, Nixon SN, Zhou ZY, Heatley F, Ashford M, Mosquera V, Attwood D, Booth C (2006) Micellization and drug solubilization in aqueous solutions of a diblock copolymer of ethylene oxide and phenyl glycidyl ether. Langmuir 22:7465–7470. doi:10.1021/la060684+
45. Gottlieb HE, Kotlyar V, Nudelman A (1997) NMR Chemical shifts of common laboratory solvents as trace impurities. J Org Chem 62:7512–7515. doi:S0022-3263(97)01176-6
46. Bossev DP, Matsumoto M, Makahara M (2000) ^{19}F NMR study of molecular aggregation of lithium perfluorooctylsulfonate in water at temperatures from 30 to 250 °C. J Phys Chem B 104:155–158. doi:10.1021/jp993047j
47. Bühler G, Feldmann C (2006) Microwave-assisted synthesis of luminescent LaPO4:Ce, Tb nanocrystals in ionic liquids. Angew Chem Int Ed 45:4864–4867. doi:10.1002/anie.200600244
48. Ilmain F, Tanaka T, Kokufuta E (1991) Volume transition in a gel driven by hydrogen bonding. Nature 349:400–401. doi:10.1038/349400a0
49. Deng L, Wang CH, Li ZC, Liang DH (2010) Re-examination of the "zipper effect" in hydrogen-bonding complexes. Macromolecules 43:3004–3010. doi:10.1021/ma902601d
50. Madsen J, Arms SP (2009) Preparation and aqueous solution properties of thermoresponsive biocompatible AB diblock copolymers. Biomacromolecules 10:1875–1887. doi:10.1021/bm9002915
51. Lombardo D, Micali N, Villari V, Kiselev MA (2004) Large structures in diblock copolymer micellar solution. Phys Rew E 70:21402–21408. doi:10.1103/PhysRevE.70.021402
52. Lobry L, Micali N, Mallamace F, Liao C, Chen SH (1999) Interaction and percolation in the *L*64 triblock copolymer micellar system. Phys Rev E 60:7076–7087. doi:10.1103/PhysRevE.60.7076